ChemCatChem

Research Article
doi.org/10.1002/cctc.202400792

Chemistry Europe
European Chemical Societies Publishing

www.chemcatchem.org

Insights into the Mechanism of a Vanadium Bromoperoxidase from the Marine Macro-Algae *Corallina pilulifera* for Biocatalytic Halogenation

Daniel E. Mitchell,[a] Esther Garcia-Rodriguez,[a] Michail N. Isupov,*[a] and Jennifer A. Littlechild*[a]

Vanadium haloperoxidases have been studied to understand their mechanism and halide specificity. Crystal structures of vanadium bromoperoxidase enzyme complexes from *Corallina piluifera*, with vanadate and bromide and with phosphate and chloride, show significant displacement of loop residues 336–338 upon halogen binding. This shows a "closed position" of Leu337 locking the bromide ion in a hydrophobic environment favoring the vanadium peroxide reaction with the halogen by retaining the resulting hypobromite in the enzyme active site. The bound cofactor exists as a mixture of free vanadate and histidine553-vanadate adduct. A mutant enzyme Arg397Trp also has been crystallized with bound phosphate and its structure determined with and without the bound bromide ion. The precise positions of the bromine have been determined using its anomalous signal. The bromide binding site in the mutant enzyme is displaced by 2.5 Å resulting in a mixed population of the "open" and the "closed" forms of Leu337. This allows additional chloroperoxidase activity due to re-positioning of the halogen ion 0.6 Å closer to the vanadate ion. These studies support the application of vanadium haloperoxidase enzymes for selective halogenation of important drug molecules.

1. Introduction

Halogenated compounds are important building blocks in the production of pharmaceuticals and fine chemicals. Specific halogenation of a compound changes its chemical and biological properties. Many established drug molecules are halogenated compounds. Using enzymes rather than conventional chemical synthetic techniques to produce these compounds is more sustainable and environmentally friendly.

Haloperoxidases catalyse enzymatic addition of halide to nucleophilic organic compounds in the presence of hydrogen peroxide and function in the biosynthesis of halogenated natural products.[1] In the active site of the haloperoxidase, hydrogen peroxide reacts with the halogen ion X to form an oxidized halogen intermediate HOX (Equation 1):

$$H_2O_2 + H^+ + X^- \rightarrow H_2O + HOX \quad (1)$$

If a convenient organic nucleophile acceptor is present, a reaction occurs with HOX to form a diverse range of halogenated products.[2] Most halogenated natural products are chlorinated, brominated, or iodinated. Fluorinated compounds are rare and are produced by a non-peroxidative mechanism.[3] Identified halogenated compounds range from simple aromatic and aliphatic compounds to complex alkaloids, polyketides and even polypeptides.[1] A large majority of these natural halogenated compounds have been isolated from marine organisms.[4] Macro-algae and cyanobacteria, in particular, appear to play an important role in the cycling of iodine and bromine in coastal waters.[5] Lichens and fungi have also been found to be a source of haloperoxidase activity and can produce organic halogenated compounds.[6–8] Many of the natural compounds identified have antibacterial or anticancer activities so in themselves form a basis for new drug molecules.

The haloperoxidase enzymes were initially classified as heme or non-heme enzymes.[9] The latter can be split into vanadium dependent[10] and cofactor-free haloperoxidases.[11] More recently, the cofactor-free haloperoxidases found in bacteria have been reclassified as esterases, since their observed halogenation reaction, which only occurs at acidic pH, is now considered a side reaction.[12,13] Other halogen transfer enzymes that have been identified are flavin-dependent haloperoxidases, *S*-adenosyl-l-methionine-dependent chlorinases, and fluorinases. These enzymes are unrelated structurally and use different mechanisms to achieve their chemical reactions (reviewed in ref. [14]). This paper will focus on vanadium haloperoxidases.

The vanadium haloperoxidases (VHPOs) are normally named after the most electronegative ion they are able to oxidise,

[a] D. E. Mitchell, E. Garcia-Rodriguez, M. N. Isupov, J. A. Littlechild
Henry Wellcome Building for Biocatalysis, Biosciences, University of Exeter, ExeterEX4 4QD, UK
E-mail: m.isupov@exeter.ac.uk
j.a.littlechild@exeter.ac.uk

Correction added on 26 May 2025: References were renumbered.

Supporting information for this article is available on the WWW under https://doi.org/10.1002/cctc.202400792

© 2024 The Author(s). ChemCatChem published by Wiley-VCH GmbH. This is an open access article under the terms of the Creative Commons Attribution License, which permits use, distribution and reproduction in any medium, provided the original work is properly cited.

© 2024 The Author(s). ChemCatChem published by Wiley-VCH GmbH

thus a chloroperoxidase (CPO) oxidises Cl^-, Br^-, and I^- and a bromoperoxidase (BPO) only Br^- and I^-.[15] *Ascophyllum nodosum*, vanadium haloperoxidase is, however, classified as a BPO although it shows low levels of CPO activity.[16]

Apart from having applications as biocatalysts, the VHPOs have attracted attention due to their vanadium redox chemistry.[17–19] These enzymes use a vanadate VO_4 cofactor which was observed as a vanadate-histidine adduct in VHPO structures reported so far. Initially, it was hypothesized that the function of VHPOs was to produce a diffusible, oxidized halogen intermediate such as hypobromite which would halogenate organic compounds in solution. However, work by Butler and co-workers demonstrated that the kinetics of enzymatic bromination was more consistent with organic substrate halogenation within the enzyme active site.[20] The same group showed that both *Ascophyllum* and *Corallina* VHPOs could regiospecifically brominate various substrates which further extends their usefulness as biocatalysts.[21]

The first crystal structure of a VHPO, the chloroperoxidase (VCPO) from the fungus *Curvularia inaequalis* was solved by Wever and co-workers in 1996, and showed the vanadium as an essential metal cofactor bound in the form of vanadate (HVO_4^{2-}) and covalently attached to a specific histidine residue.[22,23] Since then further structures have been solved for the two vanadium bromoperoxidases (VBPOs) from the brown seaweed *A. nodosum*,[16] two red algae *Corallina* species,[24,25] and the cyanobacteria *Acaryochloris marina*.[26] Structures of VCPO from bacteria *Streptomyces sp*.[27] and vanadium iodoperoxidase (VIPO) from the bacteria *Zobellia galactanivorans* have also been reported.[15] These enzymes possess a high degree of amino acid sequence homology in their active sites which is formed by a four-helix bundle structural motif and is positioned at the bottom of a deep funnel-shaped substrate channel, approximately 15–20 Å deep.[23] The conserved vanadium binding site motif for VBPO and VCPO is P[S/A]YPSGHAT,[10] where hydrogen vanadate is bound axially to a histidine side chain in an overall trigonal bipyramidal coordination geometry.[28] The three equatorial oxygens of vanadate are hydrogen bonded to two conserved arginines, a lysine, a serine, and a backbone amide of a glycine. The high similarity of the active sites in vanadium haloperoxidases raises the question of what enzyme features are enabling stereospecific halogenation of organic compounds and are determining their different halogen selectivity.

Despite the high similarity of the VHPO active sites, they are structurally configured in a different way in various species. The active site of VCPOs and bacterial VIPO is totally formed by the amino acids belonging to a single polypeptide.[15,22,27] While *Zobelia* VIPO and the fungal *Cur. inaequalis* VCPOs are monomers, the *Streptomyces* VCPO forms a dimer. Conversely, both algal and bacterial VBPOs have active sites formed by residues from two adjacent monomers, thus their quaternary structure is a multimer of active dimers. One of *A. nodosum* VBPOs is a dimer,[16] the second one is a hexamer. *Corallina* and *Aca. marina* VBPOs form large assemblies of six active dimers (dodecamers).[24–26] Since the two four-helix bundles of the *Cur. inaequalis* VCPO domains superimpose well with the bundles of the two *Cor. officinalis* VBPO monomers to form the active dimer it was suggested that the monomeric VCPO has arisen from an ancestral enzyme by gene duplication.[24]

The amino acids that form the active site of VHPOs have been determined to be remarkably similar to three families of acid phosphatases, previously considered unrelated.[11,29] This sequence similarity has raised the question about the phosphatase activity of apo-VHPOs, and indeed, the VCPO from *Cur. inaequalis* was found to hydrolyse *p*-nitrophenol phosphate.[30] Similarly, acid phosphatases from *Salmonella* and *Shigella* in which vanadate is incorporated, have weak bromoperoxidase activity and are able to oxidize enantioselectively, a sulfide to a sulfoxide.[31,32] Furthermore, due to the high reactivity of the vanadium complex, VHPOs have also been found to oxidize sulfides to sulfoxides in the absence of halides[33,34] proving that these enzymes are very versatile for use in applied biocatalysis for a wide variety of different organic compounds. The ability of the VHPOs to be used for sustainable chemical synthesis has been demonstrated for both VBPO[35] and VCPO.[36]

Despite this great potential of VHPOs as biocatalysts, their detailed mechanisms are not fully understood. The original structure of the *Cor. officinalis* VPBO was determined using enzyme extracted from the *Corallina* red algae gathered from rock pools from the SW UK coastal regions.[37,38] Attempts to overexpress the *Cor. officinalis* enzyme in bacteria were challenging, however a method was developed to refold the protein from inclusion bodies after over-expression in *Escherichia coli*.[39] It has been possible for VBPO from a related species *Cor. pilulifera*, which grows in coastal regions of Japan, to be over-expressed in yeast and this has allowed the production of mutant enzymes to obtain further mechanistic understanding. Two mutant enzymes R397 W and R397F showed significant chloroperoxidase (CPO) activity as well as BPO activity.[40,41]

A preliminary paper on the structural interpretation of the enzyme was reported by us earlier.[42] However further analysis of the halide specificity of this enzyme has revealed important additional information described in this paper. Here, we report and interpret the conformational changes which accompany binding of halogen ions in structures of a recombinant VBPO from *Cor. pilulifera* and its mutant R397W. We also report the binding of the vanadate cofactor to the enzyme active site. The results obtained have provided further understanding of the mechanism of halogenation of organic compounds by this enzyme and identified structural factors which define its halide specificity.

2. Results and Discussion

2.1. Structural Bioinformatics

A comparison of structures between *Corallina* VBPOs and *Cur. inaequalis* VCPO has shown that one of the distinct differences in the active sites was an Arg397 (*Cor. pilulifera* numbering) which replaces a tryptophan residue at this position in VCPO. *Asc. nodosum* VBPO which shows weak VCPO activity and bacterial

© 2024 The Author(s). ChemCatChem published by Wiley-VCH GmbH

VIPO both also have Trp at this position. Extensive mutagenesis of this residue R397 of *Cor. pilulifera* VBPO to every other single amino acid has shown that two mutants R397 W and R397F have acquired some limited chloroperoxidase activity while retaining strong bromoperoxidase activity.[41] Therefore, both native *Cor. pilulifera* VBPO and its R397 W mutant were chosen for structural studies to examine the differences in their active sites which would explain these differences in halogen specificity.

2.2. Crystal Structures

Previously, the *Cor. pilulifera* VBPO has been crystallized in the same dihydrogen phosphate conditions used for structure determination of the *Cor. officinalis* VBPO, with both proteins sharing 90% sequence identity.[43] The phosphate ion replaces vanadate in the enzyme active site, giving a phosphate enzyme complex. The hexagonal phosphate complex crystals (form 1) were robust, easily reproducible, and retained diffraction in the process of crystals soaking and cryocooling. To obtain the vanadate VBPO complex, crystallization was carried out in polyethylene glycol (PEG) conditions, similar to those reported for *Cor. officinalis* VBPO earlier.[37] However, resulting cubic VBPO crystals (form 2) had poor reproducibility, suffered twinning problems, and lost resolution upon cryocooling and ligand soaks. Co-crystallization and soaking trials with known organic ligand, methyl-p-tolylsulfide or HOBr scavenger phenol red and Br^- or Cl^- halogen ions were set up for both native and mutant VBPO enzymes in both crystallization conditions. However, we only managed to collect a single good data set to 2.15 Å for a complex of native VBPO in form 2 co-crystallized with KBr and soaked in methyl-p-tolylsulfide. We collected data on both native and mutant VBPOs form 1 crystals grown in the presence of both halogens and soaked with the above organic ligands.

2.3. Quality of the Structures

The four crystal structures were solved by the molecular replacement method using our previous structure of the phosphate complex of *Cor. pilulifera* VBPO as a model (pdb 1up8). In both crystal forms, the VBPO dodecamer is located on a crystallographic three-fold axis, therefore the asymmetric unit contains four protein monomers. The structures were refined to good geometry and statistical parameters (Table S1). Ramachandran outliers in some structures are glycine residues. A non-proline *cis*-peptide is formed by G484 located in the vicinity of the active site, which appears to be conserved in other VHPO structures, although the equivalent residue is Thr or Pro in other proteins. All structures contain Ca^{2+} and Na^+ ions as was previously reported for *Corallina* VBPOs.

2.4. Vanadate in VBPO Active Site

Refinement of the structure of the His553-vanadate adduct in the *Cor. pilulifera* VBPO active site of crystal form 2 resulted in a poor match of experimental electron density manifested by the presence of positive and negative difference peaks around

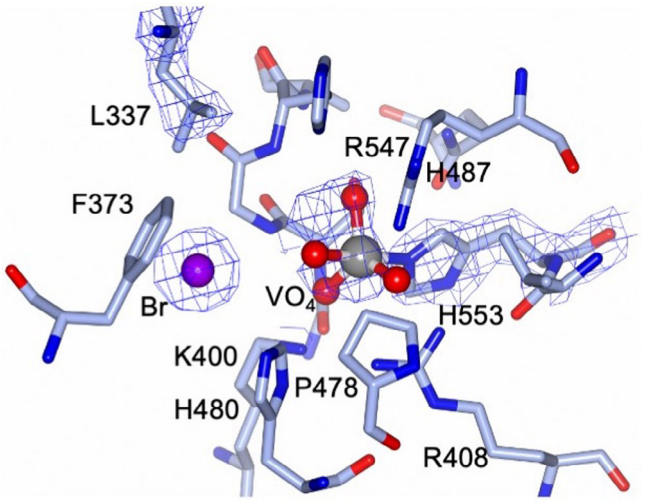


Figure 1. Wild type VBPO structure showing the active site of the *Cor. pilulifera* VBPO with bound bromine ion (purple sphere). Active site residues are shown in ice blue, while vanadate ion shown as grey (vanadium) and red (oxygen) spheres. Density map shown in blue at 1.5 sigma ($2F_0 - F_c$) and is contoured around highlighted residues. Image prepared using CCP4MG.[58]

this ligand. Alternative refinement of free vanadate VO_4 in the active site also did not show a good fit to the density. After several attempts of refinement of vanadate species at different occupancies, the structure which contains a mixture of species of vanadate histidine 553 (modelled at 30% occupancy) and free vanadate (modelled at 70% occupancy) proved to be the best description of the electron density. Both species of vanadate have similar ion pair/hydrogen bonding interactions, of which the strongest are Lys400 and Ser485. The Lys400 together with Arg547 and Arg408 can establish a protonated network around the vanadate ion and activate it towards attack by the hydrogen peroxide (Figure 1).

In each crystal structure of the VBPO, the individual monomers of the asymmetric unit are very similar with a route mean squared deviation (RMSD) in the range of 0.1–0.15 Å. However, structures of the monomers of the *Cor. pilulifera* VBPO phosphate complex (pdb 1up8) and the vanadate complex both superimpose with a RMSD of 0.38 Å over the full protein length. The active dimers superpose with a RMSD of 0.46 Å. It is not clear how much of this difference is due to the crystallization conditions and how much to the binding of a different ligand in the active site.

The vanadate in *Cur. inaequalis* VCPO and *A. nodosum* VBPO seems to bind more tightly and has been modelled as full occupancy vanadate histidine.[16,28] A low proportion of histidine vanadate can lower affinity of the cofactor for the active site and explain the complete replacement of the vanadate by phosphate. The vanadium in histidine vanadate has a trigonal bipyramidal coordination (Figure 1) and the hydrogen peroxide binding to the active was shown to replace the apical and one of the planar oxygens of histidine vanadate by peroxide as found in the peroxide form of the *Cur. inaequalis* VCPO.[28]

© 2024 The Author(s). ChemCatChem published by Wiley-VCH GmbH

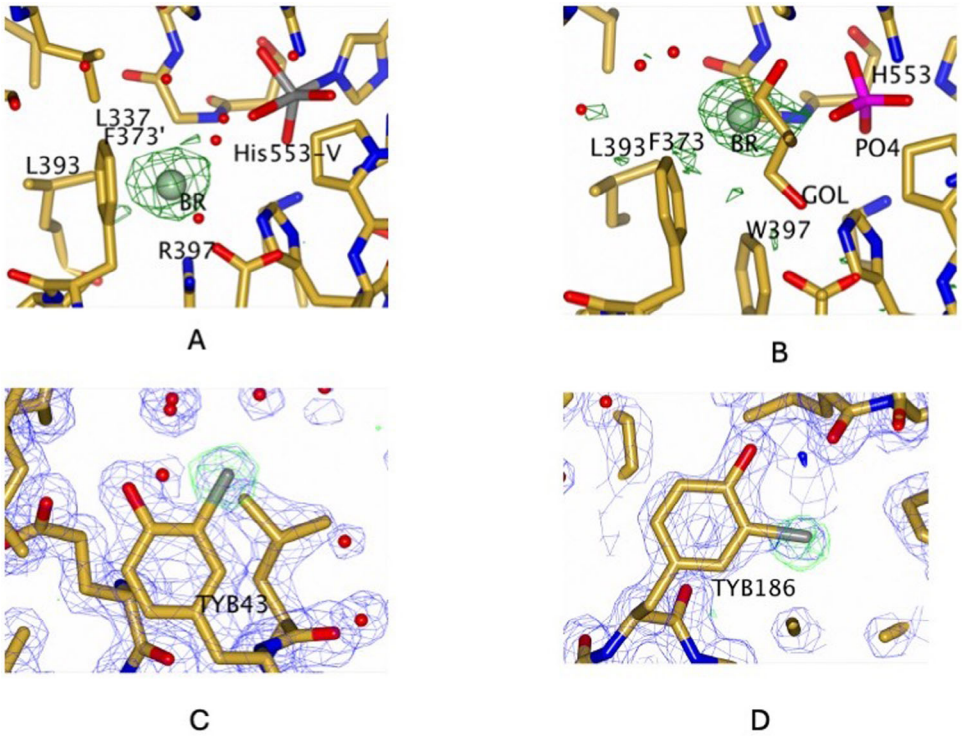


Figure 2. Location of the bromide binding and bromination sites using anomalous difference maps. Model residues are shown as sticks, anomalous difference maps are shown in green contoured at 3 σ. A) Bromide bound in the active site of WT *Cor. pilulifera* VBPO. B) Bromide bound in the active site of R397 W mutant. C) and D) Bromination of Tyr43 and Tyr186 in the R397 W mutant structure. 2Fo–Fc map is shown in blue contoured at 1.5 σ. Image prepared using CCP4MG.[58]

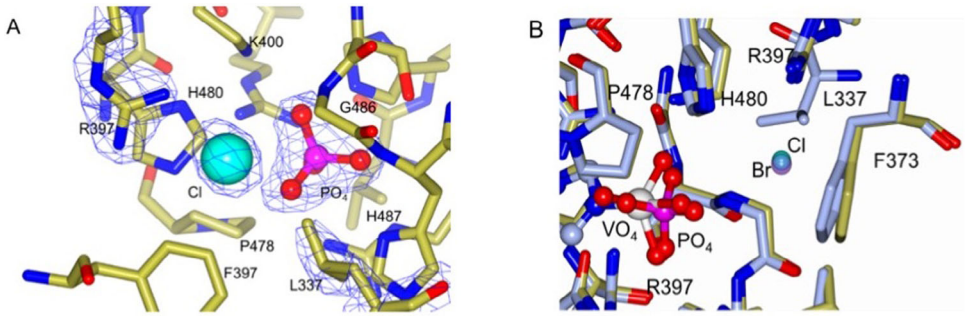


Figure 3. Structure with chloride in the active site. A) Active site showing electron density of chloride (turquoise sphere) and PO_4 (shown in pink and red). Electron density of key R397 and L337 residues are also shown. B) Comparison of vanadate and bromide structure (ice blue) and chloride and PO_4 structure (gold). Bromide shown in purple, with chloride in turquoise. The phosphate ion is shown in pink and vanadium in silver. Maps drawn to 1.5 sigma ($2F_0–F_c$). Images prepared using CCP4MG.[58]

2.5. Location of Halogen Binding Sites

Two of the four wild type and mutant structures described in this paper contain bound bromide ions and one contains chloride ions. The location of the bromides bound to protein was found from the anomalous Fourier synthesis calculated with refined model phases (Figure 2).

Since the concentration of bromide ions in the mother liquor was significant, several bromide sites with high occupancy were located within each protein monomer. The data for the wild type of enzyme chloride complex were collected at very short wavelength (0.848 Å) where the anomalous signal for this element is weak. Chloride ions were located by refinement of water molecules at these sites to extremely low B-factors and confirmed by the presence of positive difference (Fobs–Fcalc) density (Figure 3).

The bromide site in the active site of the wild type of enzyme is located close to the vanadate ion, as is visible in Figure 1. The bromide ion is coordinated by the Arg397 residue and within 3.8 Å of the closest oxygen of the vanadate-histidine adduct. Several chloride sites were located, where the position of the chloride ion in the active site is within 0.3 Å from the bromide site (Figure 3B). This is likely due to the difference of the ionic radii of the two halogens. This makes the distance of the chloride ion to nearest vanadate oxygen 3.7 Å.

© 2024 The Author(s). ChemCatChem published by Wiley-VCH GmbH

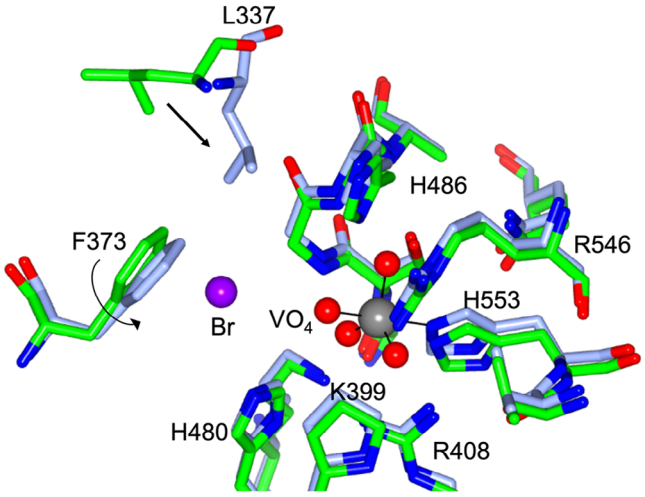


Figure 4. Comparison to previously published unbrominated complex, (pdb: 1up8, green, and brominated complex residues in ice blue). Bromide ion is shown in purple while histidine vanadate is shown as grey (vanadium) and red (oxygen) spheres. Arrows added to indicate movement of residues between the structures. Image prepared using CCP4MG.[58]

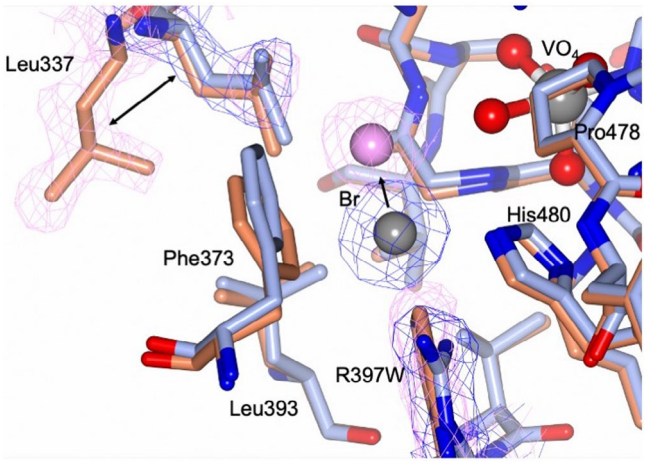


Figure 5. Comparison of the WT and R397 W structures both with bromine ions in the active site. WT in ice blue, R397 W in coral. The WT type bromide ion is shown in silver, while the R397 W bromide ion is shown in pink. The electron density maps are drawn to 1.5 sigma ($2F_0 - F_c$). The arrows added show the movement of Br and Leu337. Image prepared using CCP4MG.[58]

2.6. Active Site Rearrangement Upon Halogen Binding

Comparing the bromide and chloride complex structures of the wild type protein to the previously published structure (pdb: 1up8), a displacement of the loop containing amino acids 336–338 results in the movement of the side chain of the residue Leu337 inwards towards the active site when the halogen ion is present (Figure 4). Additionally, this displacement is accompanied by an inward movement and rotation of around 25^0 of the side chain of Phe373 from an adjacent subunit in the catalytic dimer.

In the non-halide bound structure, a water molecule occupies a similar position to the halide and Leu337 side chain. The binding of the bromide results in the formation of a hydrophobic pocket and a reduction in size of the entrance to the active site, eliminating water and allowing the reactions to occur.[30] It would appear that the hydrophobic environment that is produced by the structural rearrangement following halogen binding favors the formation of the peroxy form of histidine vanadate in the enzyme active site. This in turn results in the hypobromite formation in the VBPO active site and its retention until a suitable organic substrate binds in the deep active site cavity. Such substrate binding may cause conformational changes to the Leu337 containing loop and Phe373 and to allow opening of the active site entrance to release the hypobromite molecule to interact with the bound substrate. This agrees with the enzyme kinetics and regiospecificity reported by Butler and co-workers.[20,21]

2.7. R397W Mutant Structure

To understand which amino acids in the active site do affect the halogen specificity, further investigation was undertaken. From the wild type crystal structures and previous work of Oshiro and co-workers, it was shown that the Arg397 is involved in halogen binding.[41] Therefore, the structures of the R397 W mutant enzyme were determined both in the presence and in the absence of bromide ions.

There are few changes in the overall structure of the mutant protein. A monomer of the bromide bound form of the mutant enzyme aligns with a RMSD of 0.30 Å to the bromide form of the wild type enzyme. The difference observed between the mutant and the wild type enzyme is minimal and is less than that observed between different forms of the wild type enzyme. However, the bulky tryptophan residue displaces the bromide binding site towards the Leu337 containing loop by 2.5 Å, thereby reducing the distance from the bromide to the nearest histidine vanadate oxygen to 3.2 Å (Figure 5).

To validate our interpretation of the structural results, we have compared the different structures regarding the displacement of the bromide ion. Comparisons of the native vanadate and the R397 W mutant phosphate structures to the structure of the non-halogenated native phosphate complex of VBPO (pdb 1up8) and structures of the native vanadate Br complex (Figure S3A), the native phosphate Cl complex (Figure S3B), and the non-halogenated R387 W phosphate complex (Figure S3B) have been carried out. In all three cases, the cofactor/cofactor analogue displacements in the active site are in the range of 0.1–0.5 Å which are significantly smaller than the observed displacement of the bromide ion (2.5 Å) between the native and mutant enzyme complexes.

It appears the shorter distance between cofactor and halogen favors chloride peroxidation by this mutant enzyme as seen by us previously.[41] Interestingly, both apo and bromide containing structures of the R397W mutant enzyme have been found to have the Leu 337 loop in two conformations, corresponding to the bound (occupancy 0.3–0.4) and unbound (occupancy 0.6–0.7) states of the wild type enzyme. These occupancies seem to be little affected by bromide binding, which is no longer able

© 2024 The Author(s). ChemCatChem published by Wiley-VCH GmbH

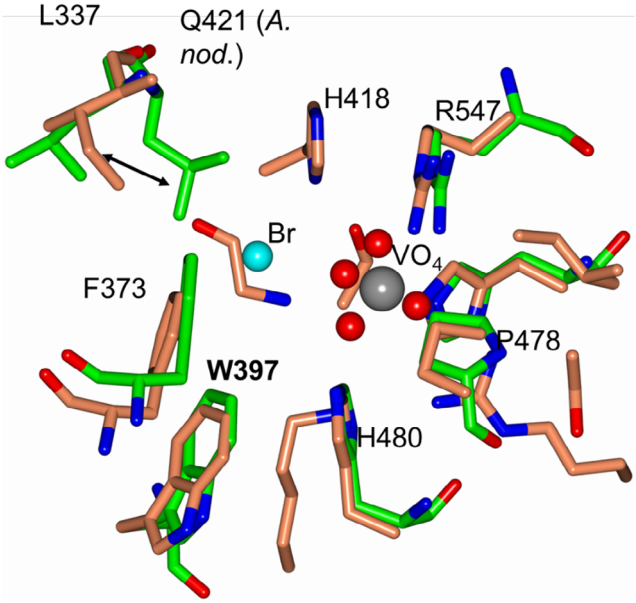


Figure 6. Comparison of R397W mutant (green) to the *A. nodosum* VBPO (coral, pdb: 1qi9). The vanadate ion from *A. nodosum* is shown as a silver sphere connected to red oxygens, while bromide from the R397 W mutant is shown as a turquoise sphere. Numbering is given using the R397 W mutant unless stated. Image prepared using CCP4MG.[58]

to bind to the "closed" conformation of the enzyme loop due to steric clashes. It would appear that the mutation R397 W has affected the proposed "lock/release" mechanism by the substrate which is no longer functional.

Clearly, halogen specificity of the haloperoxidase is an extremely important factor in the natural environment. Marine algae and bacteria have vanadium bromoperoxidase enzymes with none or limited choroperoxidase activity. It is likely chloroperoxidase activity in conditions of chloride abundance in sea water could result in production of undesired compounds. Vanadium iodoperoxidase which has a related chloroperoxidase structural fold is a further example of the importance of halogen specificity in different organisms. The content of bromine in sea water is relatively low so organisms such as *Corallina* species need to specifically sequester this for bromoperoxidase activity which has been shown to have anti-microbial properties proposed to prevent other micro-organisms colonizing the rocks that this species adhere to.

The detailed crystal structures presented in this paper suggest that the halogen to vanadate distance in the enzyme active sites is likely one of the major factors defining the different halogen specificities observed in this family of enzymes.

2.8. Structural Comparison with Related Enzymes

The R397W mutant can be compared to a similar enzyme from *A. nodosum* which also has Trp338 at the equivalent position (Figure 6). This VHPO has also been found to have activity with chlorine, however the specific activity (0.49 U/mg) was much less than that previously described for the R397W mutant.[41] A chloride ion would fit better into a smaller, more hydrophobic active site, so several amino acid residues would affect chloroperoxidase activity. It does appear however, in this case that the tryptophan plays an important role in the halide specificity.

The amino acids surrounding the vanadate ion appear to be well-conserved, however there is some difference in those surrounding the bromide ion which could account for the increased activity against chlorine in the R397 W mutant relative to *A. nodosum* enzyme The key Leu337 is replaced with a glutamine and Leu393 is likewise a glutamine in the *A. nodosum* enzyme. These differences in amino acids around the bromide ions suggest that several key amino acids within the active site play a role in halide specificity.

A structure of an iodoperoxidase from the marine bacteria *Zobellia galactanivorans* has been solved (pdb: 4cit).[15] This structure is monomeric and exhibits more structural similarity to both known VCPO structures (which are also monomeric) as opposed to the VBPO presented here. The residues His360 and Arg 410 (*Z. galactansivorans* numbering) are conserved between the VBPO and VIPO, and generally the residues coordinating the vanadate ion are extremely well conserved. Similarly to the VBPO from *A. nodosum* and a previously reported VCPO from *Cur inaequalis* (PDBiD: 1IDQ)[22] and the R397 W mutant there is a tryptophan at position 321 (Figure 7). Additionally, the residues Leu393 and Phe373 surrounding the halogen ion binding site are phenylalanine and proline, respectively, in the VIPO structure.

Likewise, in comparison with the VCPO from *Cur. Inaequalis*, the residues coordinating the vanadate cofactor are highly conserved (Figure 7). However, as observed for the comparison with the VIPO structure those residues surrounding the bromine differ, with Leu393 and Phe373 changed to glycine and proline, respectively. Given the extremely high homology of those residues surrounding the vanadate ion in all VHPOs, it is likely that a highly complex hydrogen bonding network is present involving a large number of residues. The glycine at position 346 (*Cur. inaequalis*) may provide the size and flexibility in halogen binding pocket to allow reactions to occur with chlorine, bromine, and iodine. This is supported by the work on the VIPO by Fournier et al. who managed to produce some bromoperoxidase activity on the substitution of either Ser358 or Tyr263 by an alanine residue.[15] They also found that the reason for halogen specificity was very difficult to determine and likely the result of a large number of different residues. This additionally suggests that further mutagenesis studies could be beneficial to optimize the VHPO selectivity for specific the requirements of new pharmaceutical and anti-microbial compounds.

2.9. Organic Ligand Binding

The true in vivo organic substrates of VBPO are unknown and unavailable for crystal substrate complexes. Therefore, crystals soaks were conducted with a ligand with reported in vitro activity, methyl-p-tolylsulfide and HOBr scavenger phenol red in the presence of bromide ions. A thorough investigation of the active site funnels in all the resulting crystal structures that have been determined has failed to show the presence of any of these known substrates. The active site cavities of

© 2024 The Author(s). ChemCatChem published by Wiley-VCH GmbH

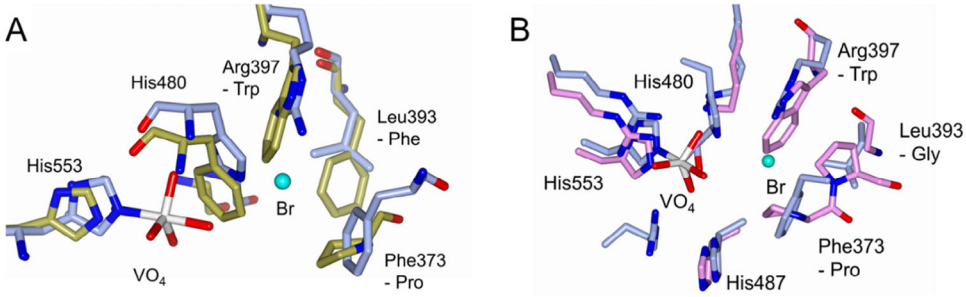


Figure 7. Comparison of active site WT *Cor. pilulifera* VBPO with bound bromine ion (ice blue residues, turquoise sphere) with A) VIPO from *Z. galactanivorans* (pdbiD: 4cit, gold residues) and B) VCPO from *Cur. inaequalis* (pdb: 1idq, pink residues). Numbering of residues is given from *Cor. pilulifera* VBPO. Image prepared using CCP4MG.[58]

the enzymes show only the presence of bound crystallization agents and cryoprotectants such as PEG, Tris buffer, and glycerol molecules. Interestingly, a recent preprint describes organic substrate binding in the cyanobacterial bromoperoxidase BPO from *Aca. marina*.[45]

2.10. Tyrosine Bromination

To avoid competition between different halogen ions for the enzyme active site, the protein was purified in Tris-HBr buffer, which resulted in bromination of two exposed tyrosine residues on the surface of the protein. (Figure 2C,D) This bromination is likely caused by diffusion of the hypobromic acid produced in the enzyme active site in the absence of suitable organic substrates. It has also been reported that *As. nodosum* VBPO also contains brominated surface Tyr residues.[46] Recent work incorporating bromo and chloro – tyrosine into glutathione S-transferase and lysozyme using the UAG stop codon, has found that proteins can be stabilized upon the incorporation of bromotyrosine at strategic locations.[47,48] This is due to halogen moieties filling internal spaces within protein molecules and in addition forming non-canonical stabilizing interactions with neighboring residues.

3. Conclusions

The first structural analysis of vanadium haloperoxidase complexes with bound halogens in the enzyme active site is presented in this paper. It was found that two key residues Leu337 and Phe373 can change their orientation to allow the formation of a suitable binding pocket for different halide specificity. This opens the opportunity to use directed mutagenesis studies to tune these enzymes for the production of novel halogenated pharmaceuticals and antimicrobials.

In addition, the structure of a R397 W mutant enzyme has been solved with and without bromide. This mutant enzyme has been found to have an enhanced activity towards chloride ions, thus broadening its halide specificity. This has given further information regarding our understanding of the halide specificity of the different vanadium haloperoxidase enzymes.

The occurrence of bromotyrosine is observed which could have a role in protein stabilization by forming interactions with neighboring residues and filling internal spaces within the protein molecule.

The VHPO enzymes clearly have important applications for applied biocatalysis involving the synthesis of novel halogenated compounds with important applications as anti-microbials and new pharmaceuticals.[49]

4. Materials and Methods

4.1. Purification of Recombinant and Mutant Enzymes

The native and mutant enzymes were kindly provided by the group of Prof Yoshi Izumi. They were produced using the yeast over-expression system as described by Ohshiro et al. in 2004.[41] The enzymes were further purified and assayed for activity as previously described.[40,41,44]

4.2. Crystal Trials

The crystallization trials with the recombinant wild type enzyme were set up using both hanging and sitting drop vapour diffusion techniques based on previously reported conditions.[37,43] Two crystal forms were obtained, one using ammonium phosphate as precipitant, a hexagonal form, and the second a cubic vanadium bound called form 2. In this study, a chloride complex of *Cor. pilulifera* VBPO crystallized in the space group $P6_3$ with unit cell a = b = 182.12 Å, c = 177.60 Å, while R397 W mutant enzyme crystallized in the same space group with unit cell a = b = 182.12 Å, c = 177.60 Å. The mutant R397 W *Cor. pilulifera* VBPO was crystallized with and without KBr, the former crystal was soaked with phenol red. The best crystals of form 2 which were only produced with the wild type enzyme was using an initial protein of 18 mg/mL in 50 mM Tris-H_2SO_4 pH 8.5, 0.4 M KBr, 1 mM Na_3VO_4, 20% (w/v) polyethylene glycol 6000 and grew in the cubic space group $P2_13$ with unit cell dimensions a = b = c = 199.60 Å. The wild type enzyme was also crystallized in high phosphate as previously described.[44] The mutant enzyme could only be crystallized in form 1 under conditions of 100 mM Tris-HBr pH 7.4, 1.3 M ammonium phosphate giving a final pH of 5.0. A cryoprotectant at 100 mM Tris- H_2SO_4, pH 8.5, 1.6 M ammonium phosphate, 25% (v/v) glycerol was used for data collection. For the wild type enzyme, crystals grown

© 2024 The Author(s). ChemCatChem published by Wiley-VCH GmbH

from polyethylene glycol 6000 a mother liquor substituting the precipitant with 25% polyethylene glycol 400 and 25% polyethylene glycol 6000 was used to allow cryocooling without formation of ice.

4.3. Crystal Soaks

Substrates used were potassium bromide, potassium chloride, phenol red, and methyl-p-tolylsulfide. These were prepared by the addition of 5% of the desired substrate to the cryoprotectant, except in the case of potassium bromide which was added at 50 mM. Optimization of soaking time was undertaken by the observation of the crystal transparency and homogeneity of the crystal faces.

4.4. Data Collection

All data was collected under cryocooled conditions at the Hamburg Synchrotron Facilities, DESY, on stations BW7A and BW7B. For native and mutant bromide complexes, the beamline wavelength was adjusted slightly below the absorption edge of the element bromine (0.9202 Å) in order to use the anomalous dispersion to locate the potential bromine ions in the structure. The crystallographic data was processed and scaled using the HKL package.[50] Molecular replacement procedures were carried out using the program AmoRe from the CCP4 package.[51] The refinement procedure was carried out using REFMAC[52] with graphical support of the program COOT.[53] The analysis of the anomalous signal was performed using CCP4 suite in CCP4cloud interface.[54] Libraries for chemically modified residues were created using the program JLigand.[55] Analysis of the quality of the data and the structure solutions were carried out using the programs SFCHECK and Molprobity.[56,57]

Author Contributions

Jennifer A. Littlechild initiated the project and coordinated the overall research. Esther Garcia-Rodriguez crystallized the enzyme. Daniel E. Mitchell, Esther Garcia-Rodriguez, and Michail N. Isupov carried out the structural analysis. Daniel E. Mitchell, Michail N. Isupov, and Jennifer A. Littlechild wrote the manuscript.

Acknowledgements

Daniel E. Mitchell acknowledges EPSRC grant number EP/T002875/1. Esther Garcia-Rodrguez was supported for her PhD by the University of Exeter. The original structural studies of VBPO from *Cor. officinalis* were supported by a BBSRC programme grant 'The Exploitation of Vanadium Haloperoxidase Enzymes in Applied Biocatalysis' and a BBSRC Japan Travel Award to Jennifer A. Littlechild. Both Jennifer A. Littlechild and Michail N. Isupov thank the University of Exeter for general support and for any open access costs associated with this publication. Jennifer A. Littlechild especially thanks the members of the laboratory of the deceased Prof. Yoshi Izumi in Tottori, Japan, who provided recombinant *Cor. pulifera* wild type and mutant enzyme for these structural studies. The authors acknowledge support under the European Community Access to Research Infrastructure Action of the Improving Human Potential Programme to EMBL Hamburg Outstation, contract number HPRI-CT-1999-00017. The authors thank beamline scientists of EMBL Hamburg Outstation for useful discussion. The authors would also like to dedicate this paper to the memory of Prof. Yoshi Izumi and his support and active collaboration on the VBPO enzymes.

Conflict of Interests

The authors declare no conflict of interest.

Data Availability Statement

The data that support the findings of this study are openly available in Protein Data Bank at https://doi.org/10.2210/pdb7qwi/pdb, reference number 81959.

Keywords: Biocatalytic halogenation · Enzyme Mechanism · Halogen specificity · Vanadium bromoperoxidase

[1] G. W. Gribble, *Chemosphere* **2003**, *52*, 289–297.
[2] A. Butler, *Curr. Opin. Chem. Biol.* **1998**, *2*, 279–285.
[3] F. H. Vaillancourt, E. Yeh, D. A. Vosburg, S. Garneau-Tsodikova, C. T. Walsh, *Chem. Rev.* **2006**, *106*, 3364–3378.
[4] D. J. Faulkner, *Nat. Prod. Rep.* **2002**, *19*, 1–49.
[5] M. W. Carrano, K. Yarimizu, J. L. Gonzales, R. Cruz-López, M. S. Edwards, T. M. Tymon, F. C. Küpper, C. J. Carrano, *Algae* **2020**, *35*, 167–176.
[6] N. Bar-Nun, S. Shcolnick, A. M. Mayer, *FEMS Microbiol. Lett.* **2002**, *217*, 121–124.
[7] S. Raugei, P. Carloni, *J. Phys. Chem. B.* **2006**, *110*, 3747-3758.
[8] H. Plat, B. E. Krenn, R. Wever, *Biochem. J.* **1987**, *248*, 277–279.
[9] J. A. Manthey, L. P. Hager, *Biochemistry* **1989**, *28*, 3052-3057.
[10] C. Leblanc, H. Vilter, J. B. Fournier, L. Delage, P. Potin, E. Rebuffet, G. Michel, P. L. Solari, M. C. Feiters, M. Czjzek, *Coord. Chem. Rev.* **2015**, *301–302*, 134–146.
[11] W. Hemrika, R. Renirie, H. L. Dekker, P. Barnett, R. Wever, *Proc. Natl. Acad. Sci. USA* **1997**, *94*, 2145–2149.
[12] B. Hofmann, S. Tölzer, I. Pelletier, J. Altenbuchner, K. H. van Pée, H. J. Hecht, *J. Mol. Biol.* **1998**, *279*, 889–900.
[13] K. Line, M. N. Isupov, J. A. Littlechild, *J. Mol. Biol.* **2004**, *338*, 519–532.
[14] A. Hill, J. Littlechild, in *Comprehensive Chirality* (Eds E. M. Carreira, H. Yamamoto), Elsevier, Amsterdam, **2012**, *7*, pp 329–349.
[15] J.-B. Fournier, E. Rebuffet, L. Delage, R. Grijol, L. Meslet-Cladière, J. Rzonca, P. Potin, G. Michel, M. Czjzek, C. Leblanc, *Appl. Environ. Microbiol.* **2014**, *80*, 7561–7573.
[16] M. Weyand, H. Hecht, M. Kiess, M. Liaud, H. Vilter, D. Schomburg, *J. Mol. Biol.* **1999**, *293*, 595–611.
[17] G. J. Colpas, B. J. Hamstra, J. W. Kampf, V. L. Pecoraro, *J. Am. Chem. Soc.* **1996**, *118*, 3469–3478.
[18] J. Littlechild, *Curr. Opin. Chem. Biol.* **1999**, *3*, 28–34.
[19] J. M. Winter, B. S. Moore, *J. Biol. Chem.* **2009**, *284*, 18577–18581.
[20] R. A. Tschirret-Guth, A. Butler, *J. Am. Chem. Soc.* **1994**, *116*, 411–412.

© 2024 The Author(s). ChemCatChem published by Wiley-VCH GmbH

[21] J. S. Martinez, G. L. Carroll, R. A. Tschirret-Guth, G. Altenhoff, R. D. Little, A. Butler, *J. Am. Chem. Soc.* **2001**, *123*, 3289–3294.
[22] A. Messerschmidt, R. Wever, *Proc. Nat. Acad. Sci USA* **1996**, *93*, 392–396.
[23] S. Macedo-Ribeiro, W. Hemrika, R. Renirie, R. Wever, A. Messerschmidt, *J. Biol. Inorg. Chem.* **1999**, *4*, 209–219.
[24] M. N. Isupov, A. R. Dalby, A. A. Brindley, Y. Izumi, T. Tanabe, G. N. Murshudov, J. A. Littlechild, *J. Mol. Biol.* **2000**, *299*, 1035–1049.
[25] E. Garcia-Rodriguez, T. Ohshiro, T. Aibara, Y. Izumi, J. Littlechild, *J. Biol. Inorg. Chem.* **2005**, *10*, 275–282.
[26] A. Frank, C. J. Seel, M. Groll, T. Gulder, *ChemBioChem* **2016**, *17*, 2028–2032.
[27] P. Y. Chen, S. Adak, J. R. Chekan, D. K. Liscombe, A. Miyanaga, P. Bernhardt, S. Diethelm, E. N. Fielding, J. H. George, Z. D. Miles, L. A. M. Murray, T. S. Steele, J. M. Winter, J. P. Noel, B. S. Moore, *Biochemistry* **2022**, *61*, 1844–1852.
[28] A. Messerschmidt, L. Prade, R. Wever, *Biol. Chem.* **1997**, *378*, 309–316.
[29] A. F. Neuwald, *Protein Sci.* **1997**, *6*, 1764–1767.
[30] R. Renirie, W. Hemrika, R. Wever, *J. Biol. Chem.* **2000**, *275*, 11650–11657.
[31] C. M. Vescina, V. C. Sálice, A. M. Cortizo, S. B. Etcheverry, *Biol. Trace. Elem. Res.* **1996**, *53*, 185–191.
[32] N. Tanaka, V. Dumay, Q. Liao, A. J. Lange, R. Wever, *Eur. J. Biochem.* **2002**, *269*, 2162–2167.
[33] M. Andersson, A. Willetts, S. Allenmark, *J. Org. Chem.* **1997**, *62*, 8455–8458.
[34] J. Littlechild, E. Garcia-Rodriguez, A. Dalby, M. Isupov, *J. Mol. Recognit.* **2002**, *15*, 291–296.
[35] D. Wischang, M. Radlow, J. Hartung, *DaltonTrans.* **2013**, *42*, 11926–11940.
[36] S. H. H. Younes, F. Tieves, D. Lan, Y. Wang, P. Süss, H. Brundiek, R. Wever, F. Hollmann, *ChemSusChem* **2020**, *13*, 97–101.
[37] C. Rush, A. Willetts, G. Davies, Z. Dauter, H. Watson, J. Littlechild, *FEBS Lett.* **1995**, *359*, 244–246.
[38] E. Garcia-Rodriguez, *PhD Thesis*, University of Exeter (UK), **2005**.
[39] E. E. Coupe, M. G. Smyth, A. P. Fosberry, R. M. Hall, J. A. Littlechild, *Protein Expr. Purif.* **2007**, *52*, 265–272.
[40] T. Ohshiro, W. Hemrika, T. Aibara, R. Wever, Y. Izumi, *Phytochemistry* **2002**, *60*, 595–601.
[41] T. Ohshiro, J. Littlechild, E. Garcia-Rodriguez, M. N. Isupov, Y. Iida, T. Kobayashi, Y. Izumi, *Protein Sci.* **2004**, *13*, 1566–1571.
[42] J. Littlechild, E. Garcia Rodriguez, M. Isupov, *J. Inorg. Biochem.* **2009**, *103*, 617-621.
[43] A. A. Brindley, A. R. Dalby, M. N. Isupov, J. A. Littlechild, *Acta Crystallogr. Sect. D Biol. Crystallogr.* **1998**, *54*, 454–457.
[44] J. Littlechild, E. Garcia-Rodriguez, *Coord. Chem. Rev.* **2003**, *237*, 65–76.
[45] T. Gulder, P. Zeides, K. Bellmann-Sickert, R. Zhang, C. Seel, V. Most, C. Schoeder. M. Groll, Chemrxiv, **2023**, https://doi.org/10.26434/chemrxiv-2023-7l30h.
[46] M. C. Feiters, C. Leblanc, F. C. Küpper, W. Meyer-Klaucke, G. Michel,P. Potin, *J. Am Chem. Soc.* **2005**, *127*, 15340–15341.
[47] K. Ohtake, A. Yamaguchi, T. Mukai, H. Kashimura, N. Hirano, M. Haruki, S. Kohashi, K. Yamagishi, K. Murayama, Y. Tomabechi, T. Itagaki, R. Akasaka, M. Kawazoe, C. Takemoto, M. Shirouzu, S. Yokoyama, K. Sakamoto, *Sci. Rep.* **2015**, *5*, 9762.
[48] A.-C. C. Carlsson, M. R. Scholfield, R. K. Rowe, M. C. Ford, A. T. Alexander, R. A. Mehl, P. S. Ho, *Biochemistry* **2018**, *57*, 4135–4147.
[49] J. Littlechild, M. Isupov, In: *Recent Advances in Redox Active Plant and Microbial Products: From Basic Chemistry to Widespread Applications in Medicine and Agriculture*. (Eds.: C. Jacob, G. Kirsch, A. Slusarenko, P. G. Winyard, T. Burkholz) Dordrecht: Springer, Netherlands. **2014** pp. 425–446.
[50] Z. Otwinowski, W. Minor, *Methods Enzymol* **1997**, *276*, 307–326.
[51] M. D. Winn, C. C. Ballard, K. D. Cowtan, E. J. Dodson, P. Emsley, P. R. Evans, R. M. Keegan, E. B. Krissinel, A. G. Leslie, A. McCoy, S. J. McNicholas, G. N. Murshudov, N. S. Pannu, E. A. Potterton, H. R. Powell, R. J. Read, A. Vagin, K. S. Wilson, *Acta Crystallogr. Sect. D Biol. Crystallogr.* **2011**, *67*, 235–242.
[52] G. N. Murshudov, P. Skubák, A. A. Lebedev, N. S. Pannu, R. A. Steiner, R. A. Nicholls, M. D. Winn, F. Long, A. A. Vagin, *Acta Crystallogr. D Biol. Crystallogr.* **2011**, *67*, 355–367.
[53] P. Emsley, B. Lohkamp, W. G. Scott, K. Cowtan, *Acta Crystallogr. D Biol. Crystallogr.* **2010**, *66*, 486–501.
[54] E. Krissinel, A. A. Lebedev, V. Uski, C. B. Ballard, R. M. Keegan, O. Kovalevskiy, R. A. Nicholls, N. S. Pannu, P. Skubák P, J. Berrisford, M. Fando, B. Lohkamp, M. Wojdyr, A. J. Simpkin, J. M. H. Thomas, C. Oliver, C. Vonrhein, G. Chojnowski, A. Basle, A. Purkiss, M. N. Isupov, S. McNicholas, E. Lowe, J. Triviño, K. Cowtan, J. Agirre, D. J. Rigden, I. Uson, V. Lamzin, I. Tews, G. Bricogne, A. G. W. Leslie, D. G. Brown, *Acta Crystallogr. D Struct. Biol.* **2022** *78*, 1079–1089.
[55] A. A. Lebedev, P. Young, M. N. Isupov, O. V. Moroz, A. A. Vagin, G. N. Murshudov, *Acta Crystallogr. D Biol. Crystallogr.* **2012** *68*, 431–440.
[56] A. A. Vaguine, J. Richelle, S. J. Wodak, *Acta Crystallogr. Sect. D Biol. Crystallogr.* **1999**, *55*, 191–205.
[57] C. J. Williams, J. J. Headd, N. W. Moriarty, M. G. Prisant, L. L. Videau, L. N. Deis, V. Verma, D. A. Keedy, B. J. Hintze, V. B. Chen, S. Jain, S. M. Lewis, W. B. Arendall, J. Snoeyink, P. D. Adams, S. C. Lovell, J. S. Richardson, D. C. Richardson, *Protein Sci.* **2018**, *27*, 293–315.
[58] S. McNicholas, E. Potterton, K. S. Wilson, M. E. Noble, *Acta Crystallogr. Sect. D Biol. Crystallogr.* **2011**, *67*, 386–394.

Manuscript received: May 01, 2024
Revised manuscript received: October 22, 2024
Accepted manuscript online: November 12, 2024
Version of record online: November 19, 2024

© 2024 The Author(s). ChemCatChem published by Wiley-VCH GmbH